International Journal of Applied Science and Engineering
2015. 13, 1: 19-35

Buckling Analysis of Functionally Graded Plates Using Higher Order Shear Deformation Theory with Thickness Stretching Effect

Bathini Sidda Reddy[a*], Jyothula Suresh Kumar[b], Chevireddy Eswara Reddy[c] and Kondakkagari Vijaya Kumar Reddy[b]

[a] *School of Mechanical Engineering, RGMCET, Nandyal, Kurnool (Dt), A.P, India*
[b] *Department of Mechanical Engineering, J.N.T.U.H. College of Engineering, J.N, India*
[c] *Director, The School of Engineering & Technology, SPMVV, Women's University, Tirupati, Chittoor (Dt) A.P, India*

Abstract: The prime aim of the present study is to present analytical formulations and solutions for the buckling analysis of simply supported functionally graded plates (FGPs) using higher order shear deformation theory (HSDT). This study considers the thickness stretching effect and non-zero transverse shear stresses conditions on the top and bottom surfaces of the plate. It does not require shear correction factors. Material properties of the plate are assumed to vary in the thickness direction according to a power law distribution in terms of the volume fractions of the constituents. The equations of equilibrium and boundary conditions are derived using the principle of virtual work. Solutions are obtained for FGPs in closed-form using Navier's technique. Comparison studies are performed to verify the validity of the present results from which it can be concluded that the proposed theory is accurate and efficient in predicting the buckling behavior of functionally graded plates. The effect of side-to-thickness ratio, aspect ratio, modulus ratio, the volume fraction exponent and the loading conditions on the critical buckling load of FGPs is also investigated and discussed.

Keywords: Functionally graded plates; thickness stretching effect; higher order shear deformation theory; Navier's method closed form solutions; buckling analysis.

1. Introduction

Functionally graded materials (FGMs) are the new generation of novel composite materials in the family of engineering composites, whose properties are varied smoothly in the spatial direction microscopically to improve the overall structural performance. These materials offer great promise in high temperature environments, for example, wear-resistant linings for handling large heavy abrasive ore particles, rocket heat shields, heat exchanger tubes, thermo-electric generators, heat engine components, plasma facings for fusion reactors, and electrically insulating metal/ceramic joints and also these are widely used in many structural applications such as mechanics, civil engineering, optical, electronic, chemical, mechanical, biomedical, energy sources, nuclear, automotive fields and ship building industries to minimize

* Corresponding author; e-mail: bsrrgmcet@gmail.com
Received 3 september 2013
Revised 9 october 2014
Accepted 20 November 2014

thermomechanical mismatch in metal-ceramic bonding. Most structures, irrespective of their use, will be subjected to dynamic loads during their operational life. Increased use of FGMs in various structural applications necessitates the development of accurate theoretical models to predict their response.

In the past, a variety of plate theories have been proposed to study the buckling behavior of FGM plates. The Classical plate theory (CPT) provides acceptable results only for the analysis of thin plates and neglects the transverse shear effects. Javaheri and Eslami [1], Abrate [2], Mohammadi et al.[3], Mahdavian [4], Feldman and Aboudi [5], Shariat et al. [6], Tung and Duc [7] were employed this theory to analyze buckling behavior of FG plates. However, for moderately thick plates CPT under predicts deflections and over predicts buckling loads and natural frequencies. The first-order shear deformation theories (FSDTs) are based on Reissner [8] and Mindlin [9] accounts for the transverse shear deformation effect by means of a linear variation of in-plane displacements and stresses through the thickness of the plate, but requires a correction factor to satisfy the free transverse shear stress conditions on the top and bottom surfaces of the plate. Although, the FSDT provides a sufficiently accurate description of response for thin to moderately thick plates, it is not convenient to use due to difficulty with determination of the correct value of shear correction factor [10].

The authors [11-16] used FSDT to analyze the buckling of FG plates. In-order to overcome the limitations of FSDT many HSDTs were developed that involve higher order terms in Taylors expansions of the displacements in the thickness coordinate. Javaheri and Eslami [17], Najafizadeh and Heydari [18], Bodaghi and Saidi [19], Bagherizadeh et al. [20], Mozafari and Ayob [21] were used the HSDT to analyze the buckling behavior of FG plates. Ma and Wang [22] have investigated the axisymmetric large deflection bending and post-buckling behavior of a functionally graded circular plate under mechanical, thermal and combined thermal-mechanical load based on classical nonlinear von Karman plate theory. They observed from their investigation that the power law index “n” has a significant effect on the mid-plane temperature, critical buckling temperature and on the thermal post-buckling behavior of FGM plate.

Hosseini-Hashemi et al. [23] have developed the closed-form solutions in analytical form to study the buckling behavior of in-plane loaded isotropic rectangular FG plates without any use of approximation for different boundary conditions using the Mindlin plate theory. Saidi et al. [24] employed the unconstrained third-order shear deformation theory to analyze the axisymmetric bending and buckling of FG solid circular plates in which the bending-stretching coupling exists. Oyekoya et al. [25] developed Mindlin-type and Ressner type element for modeling of FG composite plate subjected to buckling and free vibration. Further, they studied the plate for the effect of different fiber distribution cases and the effects of fire distribution on buckling and free vibration.

Ghannadpour et al. [26] applied finite strip method to analyze the buckling behavior of rectangular FG plats under thermal load. The solution was obtained by the minimization of the total potential energy and solving the corresponding eigenvalue problem. Thai and Choi [27] presented a simple refined theory to analyze the buckling behavior of FG plates which has strong similarity with classical plate theory in many aspects, accounts for a quadratic variation of the transverse shear strains across the thickness and satisfies the zero traction boundary conditions on the top and bottom surfaces of the plate without using shear correction factors. The governing equations were derived from the principle of minimum total potential energy. The effects of loading conditions and variations of power of functionally graded material, modulus ratio, aspect ratio, and thickness ratio were also investigated by these authors.

Thai and Vo [10] have developed a new sinusoidal shear deformation theory to study the

bending, buckling and vibration of FG plates accounting for sinusoidal distribution of transverse shear stress and satisfies the free transverse shear stress conditions on the top and bottom surfaces of the plate without using shear correction factor. Uymaz and Aydogdu [28] analyzed the rectangular FG plates under different axial loadings for buckling based on small strain elasticity theory with different boundary conditions. They also investigated the effects of the different material composition and the plate geometry on the critical buckling loads and mode shapes.

Lal et al. [29] have examined the second order statistics of post buckling responses of FGM plate subjected to mechanical and thermal load with non-uniform temperature changes subjected to temperature independent and dependent material properties. The effect of random material properties with amplitude ratios, volume fraction index, plate thickness ratios, aspect ratios, boundary conditions and types of loadings subjected to temperature independent and temperature dependent material properties were investigated through numerical examples.

This paper aims to develop analytical formulations and solutions for the buckling analysis of functionally graded plates (FGPs) using higher order shear deformation theory (HSDT) accounting the thickness stretching effect and without enforcing zero transverse shear stress on the top and bottom surfaces of the plate. This doesnot require shear correction factor. The plate material is graded through the thickness direction. The plate's governing equations and its boundary conditions are derived by employing the principle of virtual work. Solutions are obtained for FGPs in closed-form using Navier's technique and solving the eigenvalue equation. The present results are compared with the solutions of the Thai and Choi [27] to study the effect of thickness stretching in predicting the critical buckling loads of FG plates. The effect of side-to-thickness ratios, aspect ratios and modulus ratios and the volume fraction exponent on the critical buckling loads are studied after establishing the accuracy of the present results for FG plates.

2. Theoretical formulation

In formulating the higher-order shear deformation theory, a rectangular plate of length a, width b and thickness h is considered, that composed of functionally graded material through the thickness. Figure 1 shows the functionally graded material plate with the rectangular Cartesian coordinate system x, y and z. The material properties are assumed to be varied in the thickness direction only and the bright and dark areas correspond to ceramic and metal particles respectively. On the top surface (z=+h/2), the plate is composed of full ceramic and graded to the bottom surface (z=-h/2) that composed of full metal. The reference surface is the middle surface of the plate (z=0). The functionally graded material plate properties are assumed to be the function of the volume fraction of constituent materials. The functional relationship between the material property and the thickness coordinates is assumed to be

$$P(z) = (P_t - P_b)\left(\frac{z}{h} + \frac{1}{2}\right)^n + P_b \quad (1)$$

Where P denoted\s the effective material property, Pt, and Pb denotes the property on the top and bottom surface of the plate respectively and n is the material variation parameter that dictates the material variation profile through the thickness. The effective material properties of the plate, including Young's modulus, E, density, ρ, and shear modulus, G, vary according to equations (1) and poisons ratio (υ) is assumed to be constant.

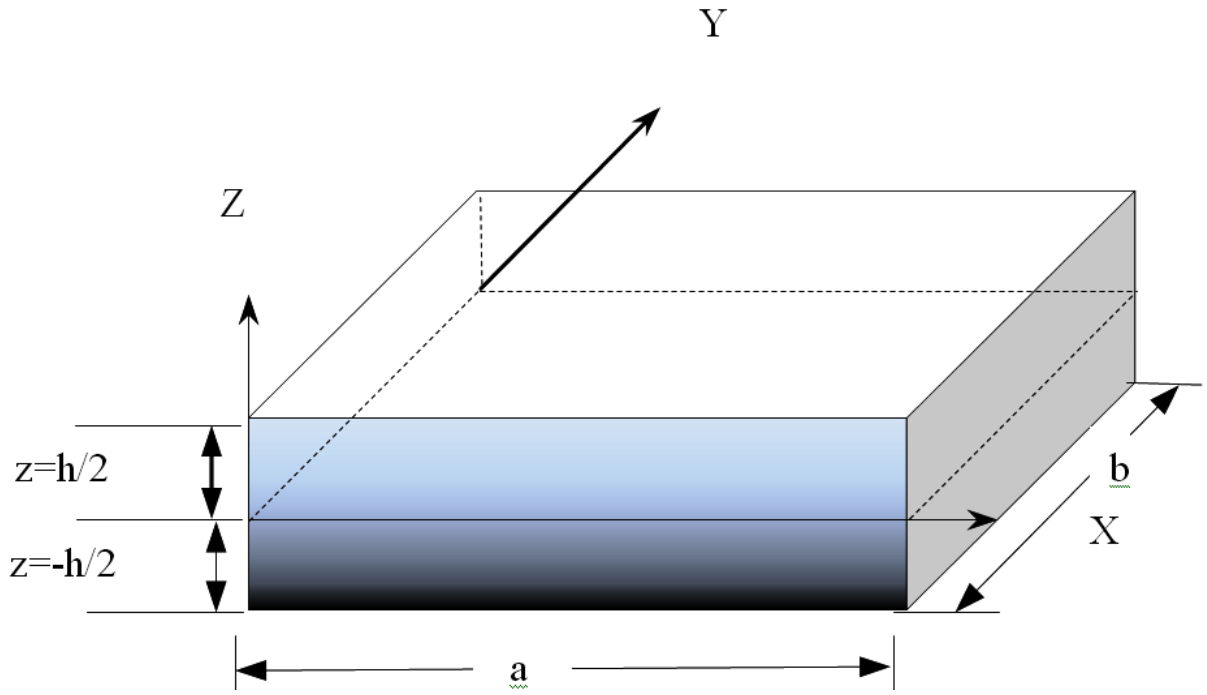

Figure 1. Functionally graded plate and coordinates

2.1. Displacement models

In order to approximate 3D plate problem to a 2D one, the displacement components u (x, y, z, t), v (x, y, z, t) and w (x, y, z, t) at any point in the plate are expanded in terms of the thickness coordinate. The elasticity solution indicates that the transverse shear stress varies parabolically through the plate thickness. This requires the use of a displacement field, in which the in-plane displacements are expanded as cubic functions of the thickness coordinate. In addition, the transverse normal strain may vary nonlinearly through the plate thickness. The displacement field which satisfies the above criteria may be assumed in the form:

$$\left.\begin{aligned} u(x,y,z) &= u_o(x,y) + z\theta_x(x,y) + z^2 u_o^*(x,y) + z^3\theta_x^*(x,y) \\ v(x,y,z) &= v_o(x,y) + z\theta_y(x,y) + z^2 v_o^*(x,y) + z^3\theta_y^*(x,y) \\ w(x,y,z) &= w_o(x,y) + z\theta_z(x,y) + z^2 w_o^*(x,y) + z^3\theta_z^*(x,y) \end{aligned}\right\} \quad (2)$$

Where u_0, v_0 is the in-plane displacements of a point (x, y) on the mid plane;

w_o is the transverse displacement of a point (x, y) on the mid plane;

θ_x, θ_y , θ_z are rotations of the normal to the mid plane about y and x–axes;

u_0^*, v_0^*, w_0^*, θ_x^*, θ_y^*, and θ_z^* are the corresponding higher order deformation terms.

By substitution of displacement relations from equations (2) into the strain displacement equations of the classical theory of elasticity the following relations are obtained:

$$\varepsilon_X = \varepsilon_{XO} + zk_X + z^2\varepsilon_{XO}^* + z^3 k_X^*$$

$$\varepsilon_y = \varepsilon_{yO} + zk_y + z^2\varepsilon_{yO}^* + z^3 k_y^*$$

$$\begin{aligned}
\varepsilon_z &= \varepsilon_{zo} + zk_z + z^2\varepsilon_{zo}^* \\
\gamma_{xy} &= \varepsilon_{xyo} + zk_{xy} + z^2\varepsilon_{xyo}^* + z^3k_{xy}^* \\
\gamma_{yz} &= \phi_y + zK_{yz} + z^2\phi_y^* + z^3k_{yz}^* \\
\gamma_{xz} &= \phi_x + zK_{xz} + z^2\phi_x^* + z^3k_{xz}^*
\end{aligned} \tag{3}$$

Where

$$\varepsilon_{xo} = \frac{\partial uo}{\partial x},\ \varepsilon_{yo} = \frac{\partial vo}{\partial y},\ \varepsilon_{xyo} = \frac{\partial uo}{\partial y} + \frac{\partial vo}{\partial x},\ \varepsilon_{z0} = \theta_z, k_z = 2w_0^*,\ \mathrm{k_x} = \frac{\partial \theta_x}{\partial x},$$

$$\mathrm{k_y} = \frac{\partial \theta_y}{\partial y},\ \mathrm{k_{xy}} = \frac{\partial \theta_x}{\partial y} + \frac{\partial \theta_y}{\partial x},\ \mathrm{k_x^*} = \frac{\partial \theta_x^*}{\partial x},\ \mathrm{k_y^*} = \frac{\partial \theta_y^*}{\partial y},\ \mathrm{k_{xy}^*} = \frac{\partial \theta_x^*}{\partial y} + \frac{\partial \theta_y^*}{\partial x},$$

$$\varepsilon_{xo}^* = \frac{\partial \mathrm{u_o^*}}{\partial x},\ \varepsilon_{yo}^* = \frac{\partial \mathrm{v_o^*}}{\partial y},\ \varepsilon_{xyo}^* = \frac{\partial \mathrm{u_o^*}}{\partial y} + \frac{\partial \mathrm{v_o^*}}{\partial x},\ \varepsilon_{z0}^* = 3\theta_z^*, \phi_y = \theta y + \frac{\partial wo}{\partial y},\ \phi_x = \theta x + \frac{\partial wo}{\partial x},$$

$$\phi_x^* = 3\theta x^* + \frac{\partial w_0^*}{\partial x},\ k_{xz}^* = \frac{\partial \theta z^*}{\partial x},\ \mathrm{k_{xz}} = 2\mathrm{u_o^*} + \frac{\partial \theta z}{\partial x},\ \phi_y^* = 3\theta y^* + \frac{\partial w_0^*}{\partial y},\ k_{yz}^* = \frac{\partial \theta_z^*}{\partial y},$$

$$\mathrm{k_{yz}} = 2\mathrm{v_o^*} + \frac{\partial \theta z}{\partial y}$$

2.2. Elastic stress-strain relations

The elastic stress-strain relations depend on which assumption of $\varepsilon_z \neq 0$. In the case of functionally graded materials the constitutive equations can be written as:

$$\begin{Bmatrix} \sigma_x \\ \sigma_y \\ \sigma_z \\ \tau_{xy} \\ \tau_{yz} \\ \tau_{xz} \end{Bmatrix} = \begin{bmatrix} Q_{11} & Q_{12} & Q_{13} & 0 & 0 & 0 \\ Q_{12} & Q_{22} & Q_{23} & 0 & 0 & 0 \\ Q_{13} & Q_{23} & Q_{33} & 0 & 0 & 0 \\ 0 & 0 & 0 & Q_{44} & 0 & 0 \\ 0 & 0 & 0 & 0 & Q_{55} & 0 \\ 0 & 0 & 0 & 0 & 0 & Q_{66} \end{bmatrix} \begin{Bmatrix} \varepsilon_x \\ \varepsilon_y \\ \varepsilon_z \\ \gamma_{xy} \\ \gamma_{yz} \\ \gamma_{xz} \end{Bmatrix} \tag{4}$$

Where(σ_x, σ_y, σ_z, τ_{xy}, τ_{yz}, τ_{xz}) are the stresses and ($\varepsilon_x, \varepsilon_y, \varepsilon_z$, γ_{xy}, γ_{yz}, γ_{xz}) are the strains with respect to the axes, Q_{ij}'s are the plane stress reduced elastic coefficients in the plate axes that vary through the plate thickness given by

$$Q_{11} = Q_{22} = Q_{33} = \frac{(1-\upsilon^2)E(z)}{1-3\upsilon^2-2\upsilon^3};\quad Q_{12} = Q_{13} = Q_{23} = \frac{\upsilon(1+\upsilon)E(z)}{1-3\upsilon^2-2\upsilon^3};$$

$$Q_{44} = Q_{55} = Q_{66} = \frac{E(z)}{2(1+\upsilon)};\qquad E(z) = (E_c - E_m)\left(\frac{z}{h} + \frac{1}{2}\right)^n + E_m \tag{5}$$

Where E_c is the modulus of Elasticity of the ceramic material and E_m is the modulus of elasticity of the metal.

2.3. Governing equations of motion

The work done by the actual forces in moving through virtual displacements, that are consistent with the geometric constraints of a body is set to zero to obtain the equation of motion and this is known as energy principle. It is useful in (a) deriving governing equations and the boundary conditions and (b) obtaining approximate solutions by virtual methods.
Energy principles provide alternative means to obtain the governing equations and their solutions. In the present study, the principle of virtual work is used to derive the equations of motion of functionally graded plates.
The governing equations of displacement model in Equation (2) will be derived using the dynamic version of the principle of virtual displacements, i.e.

$$\int_0^T (\delta U + \delta V - \delta K)\, dt = 0 \tag{6}$$

Where δU = virtual strain energy
δV = virtual work done by applied forces
δK = virtual kinetic energy
δU + δV = total potential energy.
The virtual strain energy, work done and kinetic energy is given by:

$$\delta U = \int_A \left\{ \int_{-h/2}^{h/2} \left[\sigma_x \delta \in_x + \sigma_y \delta \in_y + \sigma_z \delta \in_z + \tau_{xy}\, \delta\gamma_{xy} + \tau_{xz} \delta\gamma_{xz} + \tau_{yz} \delta\gamma_{yz} \right] dz \right\} dx\, dy \tag{7}$$

$$\delta V = - \int q \delta w^{+}\, dx\, dy \tag{8}$$

Where $w^{+} = w_0 + \frac{h}{2}\theta_z + \frac{h^2}{4} w_0^{*} + \frac{h^3}{8}\theta_z^{*}$ is the transverse displacement of any point on the top surface of the plate and q is the transverse load applied at the top surface of the plate.

$$\begin{aligned} \delta K = \int_A \{ \int_{-h/2}^{h/2} \rho_0 \Big[& \left(\dot{u}_0 + Z\dot{\theta}_x + Z^2 \dot{u}_0^{*} + Z^3 \dot{\theta}_x^{*}\right)\left(\delta\dot{u}_0 + Z\delta\dot{\theta}_x + Z^2 \delta\dot{u}_0^{*} + Z^3 \delta\dot{\theta}_x^{*}\right) + \\ & \left(\dot{v}_0 + Z\dot{\theta}_y + Z^2 \dot{v}_0^{*} + Z^3 \dot{\theta}_y^{*}\right)\left(\delta\dot{v}_0 + Z\delta\dot{\theta}_y + Z^2 \delta\dot{v}_0^{*} + Z^3 \delta\dot{\theta}_y^{*}\right) + \\ & (\dot{w}_0 + z\dot{\theta}_z + z^2 \dot{w}_0^{*} + z^3\, z\dot{\theta}_0^{*})(\delta\dot{w}_0 + z\delta\dot{\theta}_z + z^2 \delta\dot{w}_0^{*} + z^3\, \delta z\dot{\theta}_0^{*}) \Big]\, dz \} dx\, dy \end{aligned} \tag{9}$$

Where q = distributed load over the surface of the plate.
$\overline{N}_x$ and $\overline{N}_y$ the inplane loads perpendicular to the edges x=0; and y=0 respectively, and $\overline{N}_{xy}$ $\overline{N}_{yx}$ the distributed shear forces parallel to the edges x=0; and y=0 respectively
ρ_0 = density of plate material
$\dot{u}_0 = \partial u0 / \partial t$, $\dot{v}_0 = \partial v0 / \partial t$ etc. indicates the time derivatives

Substituting for δU, δV and δK in the virtual work statement in Equation (6) and integrating through the thickness, integrating by parts and collecting the coefficients of

$\delta u_o, \delta v_o, \delta w_o, \delta\theta_x, \delta\theta_y, \delta\theta_z, \delta u_o^*, \delta v_o^* \delta w_o^*, \delta\theta_x^*, \delta\theta_y^*, \delta\theta_z^*$ the following equations of motion are obtained.

$$\delta u_0 : \frac{\partial N_x}{\partial x} + \frac{\partial N_{xy}}{\partial y} = I_1 \ddot{u}_0 + I_2 \ddot{\theta}_x + I_3 \ddot{u}_0^* + I_4 \ddot{\theta}_x^*$$

$$\delta v_0 : \frac{\partial N_y}{\partial y} + \frac{\partial N_{xy}}{\partial x} = I_1 \ddot{v}_0 + I_2 \ddot{\theta}_y + I_3 \ddot{v}_0^* + I_4 \ddot{\theta}_y^*$$

$$\delta w_0 : \frac{\partial Q_x}{\partial x} + \frac{\partial Q_y}{\partial y} + q = I_1 \ddot{w}_0 + I_2 \ddot{\theta}_z + I_3 \ddot{w}_0^* + I_4 \ddot{\theta}_z^*$$

$$\delta\theta_x : \frac{\partial M_x}{\partial x} + \frac{\partial M_{xy}}{\partial y} - Q_x = I_2 \ddot{u}_0 + I_3 \ddot{\theta}_x + I_4 \ddot{u}_0^* + I_5 \ddot{\theta}_x^*$$

$$\delta\theta_y : \frac{\partial M_y}{\partial y} + \frac{\partial M_{xy}}{\partial x} - Q_y = I_2 \ddot{v}_0 + I_3 \ddot{\theta}_y + I_4 \ddot{v}_0^* + I_5 \ddot{\theta}_y^*$$

$$\delta\theta_z : \frac{\partial S_x}{\partial x} + \frac{\partial S_y}{\partial y} - N_z + \frac{h}{2}(q) = I_2 \ddot{w}_0 + I_3 \ddot{\theta}_z + I_4 \ddot{w}_0^* + I_5 \ddot{\theta}_z^*$$

$$\delta u_0^* : \frac{\partial N_x^*}{\partial x} + \frac{\partial N_{xy}^*}{\partial y} - 2S_x = I_3 \ddot{u}_0 + I_4 \ddot{\theta}_x + I_5 \ddot{u}_0^* + I_6 \ddot{\theta}_x^* \tag{10}$$

$$\delta v_0^* : \frac{\partial N_y^*}{\partial y} + \frac{\partial N_{xy}^*}{\partial x} - 2S_y = I_3 \ddot{v}_0 + I_4 \ddot{\theta}_y + I_5 \ddot{v}_0^* + I_6 \ddot{\theta}_y^*$$

$$\delta w_0^* : \frac{\partial Q_x^*}{\partial x} + \frac{\partial Q_y^*}{\partial y} - 2M_z + \frac{h^2}{4}(q) = I_3 \ddot{w}_0 + I_4 \ddot{\theta}_z + I_5 \ddot{w}_0^* + I_6 \ddot{\theta}_z^*$$

$$\delta\theta_x^* : \frac{\partial M_x^*}{\partial x} + \frac{\partial M_{xy}^*}{\partial y} - 3Q_x^* = I_4 \ddot{u}_0 + I_5 \ddot{\theta}_x + I_6 \ddot{u}_0^* + I_7 \ddot{\theta}_x^*$$

$$\delta\theta_y^* : \frac{\partial M_y^*}{\partial y} + \frac{\partial M_{xy}^*}{\partial x} - 3Q_y^* = I_4 \ddot{v}_0 + I_5 \ddot{\theta}_y + I_6 \ddot{v}_0^* + I_7 \ddot{\theta}_y^*$$

$$\delta\theta z^* : \frac{\partial S_x}{\partial x} + \frac{\partial S_y}{\partial y} - 3N_z^* + \frac{h^3}{8}(q) = I_4 \ddot{w}_0 + I_5 \ddot{\theta}_z + I_6 \ddot{w}_0^* + I_7 \ddot{\theta}_z^*$$

where $\tilde{N} = \overline{\mathrm{N}}_{\mathrm{x}} \frac{\partial^2 \mathrm{w}_{\mathrm{o}}}{\partial \mathrm{x}^2} + \overline{\mathrm{N}}_{\mathrm{xy}} \frac{\partial^2 \mathrm{w}_{\mathrm{o}}}{\partial \mathrm{y} \partial \mathrm{x}} + \overline{\mathrm{N}}_{\mathrm{yx}} \frac{\partial^2 \mathrm{w}_{\mathrm{o}}}{\partial \mathrm{x} \partial \mathrm{y}} + \overline{\mathrm{N}}_{\mathrm{y}} \frac{\partial^2 \mathrm{w}_{\mathrm{o}}}{\partial \mathrm{y}^2}$

Where the force and moment resultants are defined as:

$$\begin{Bmatrix} N_x & | & N_x^* \\ N_y & | & N_y^* \\ N_z & | & N_z^* \\ N_{xy} & | & N_{xy}^* \end{Bmatrix} = \sum_{L=1}^{n} \int_{-h/2}^{h/2} \begin{Bmatrix} \sigma_x \\ \sigma_y \\ \sigma_z \\ \tau_{xy} \end{Bmatrix} \left[1 \mid z^2\right] dz \tag{11}$$

$$\begin{Bmatrix} M_x & | & M_x^* \\ M_y & | & M_y^* \\ M_z & | & 0 \\ M_{xy} & | & M_{xy}^* \end{Bmatrix} = \sum_{L=1}^{n} \int_{-h/2}^{h/2} \begin{Bmatrix} \sigma_x \\ \sigma_y \\ \sigma_z \\ \tau_{xy} \end{Bmatrix} \left[Z \mid Z^3 \right] dz \tag{12}$$

and the transverse force resultants and inertias are given by:

$$\begin{Bmatrix} Q_x & | & Q_x^* \\ Q_y & | & Q_y^* \end{Bmatrix} = \sum_{L=1}^{n} \int_{-h/2}^{h/2} \begin{Bmatrix} \tau_{xz} \\ \tau_{yz} \end{Bmatrix} \left[1 \mid Z^2 \right] dz \tag{13a}$$

$$\begin{Bmatrix} S_x & | & S_x^* \\ S_y & | & S_y^* \end{Bmatrix} = \sum_{L=1}^{n} \int_{-h/2}^{h/2} \begin{Bmatrix} \tau_{xz} \\ \tau_{yz} \end{Bmatrix} \left[Z \mid Z^3 \right] dz \tag{13b}$$

$$I_1, I_2, I_3, I_4, I_5, I_6, I_7 = \int_{-h/2}^{h/2} \rho_0 (1, Z, Z^2, Z^3, Z^4, Z^5, Z^6)\ dz\ ) \tag{14}$$

The resultants in Equations (11) - (13) can be related to the total strains in Equation (4) by the following matrix:

$$: \begin{Bmatrix} N \\ N^* \\ -- \\ M \\ M^* \\ -- \\ Q \\ Q^* \end{Bmatrix} = \begin{bmatrix} A & | & B & | & 0 \\ \overline{B^t} & | & \overline{D_b} & | & \overline{0} \\ \overline{0} & | & \overline{0} & | & \overline{D_s} \end{bmatrix} \begin{Bmatrix} \varepsilon_0 \\ \varepsilon_0^* \\ -- \\ K_s \\ K^* \\ -- \\ \phi \\ \phi^* \end{Bmatrix} \tag{15}$$

Where

$$\mathrm{N} = [\mathrm{N_x}\ \ \mathrm{N_y}\ \mathrm{N_z}\ \mathrm{N_{xy}}]^t\ ;\ N^* = [\mathrm{N_x^*}\ \ \mathrm{N_y^*}\ \mathrm{N_z^*}\ \mathrm{N_{xy}^*}]^t$$

$$\mathrm{M} = [\mathrm{M_x}\ \ \mathrm{M_y}\ \mathrm{M_z}\ \ \mathrm{M_{xy}}]^t\ ;\ M^* = [\mathrm{M_x^*}\ \ \mathrm{M_y^*}\ \mathrm{M_z^*}\ \mathrm{M_{xy}^*}]^t$$

$$\mathrm{Q} = [\mathrm{Q_x}\ \ \mathrm{Q_y}\ S_x\ \ S_y]^t\ ;\ Q^* = [\mathrm{Q_x^*}\ \ Q_y^*\ \mathrm{S_x^*}\ \ \mathrm{S_y^*}]^t$$

$$\varepsilon_0 = [\varepsilon_{x0}\ \ \varepsilon_{y0}\ \ \varepsilon_{z0}\ \ \varepsilon_{xy0}]^t\ ;\varepsilon_0^* = [\varepsilon_{x0}^*\ \ \varepsilon_{y0}^*\ \ \varepsilon_{z0}^*\ \ \varepsilon_{xy0}^*]^t$$

$$K\ = [K_x\ \ K_y\ \ K_z\ K_{xy}]^t\ ;\ K^* = [K_x^*\ \ K_y^*\ \ 0\ K_{xy}^*]^t$$

$$\phi = [\phi_{\mathrm{x}}\ \ \phi_{\mathrm{y}}\ \ k_{xz}\ k_{yz}]^t\ ;\ \phi^* = [\phi_{\mathrm{x}}^*\ \ \phi_y^*\ k_{xz}^*\ \ K_{yz}^*]^t$$

The matrices [A], [B], [D] and [Ds] are the plate stiffness whose elements can be calculated using Equation (4), and Equations (11) - (13).

3. Analytical solution for the simply supported plate

Let a simply supported rectangular plate with length a and width b which is subjected to in-plane loading in two directions ($\overline{N}_x = -\lambda_1 N_{cr}, \overline{N}_y = -\lambda_2 N_{cr}, \overline{N}_{xy} = 0$). The following expressions of displacements are chosen based on the Navier's approach to automatically satisfy the simply supported boundary conditions of the plate.

$$u_0(x,y) = \sum_{m=1}^{\infty}\sum_{n=1}^{\infty} U_{mn} \cos\alpha x \sin\beta y \ , \ 0\le x\le a;\ 0\le y\le b; \tag{16a}$$

$$v_0(x,y,t) = \sum_{m=1}^{\infty}\sum_{n=1}^{\infty} V_{mn} \sin\alpha x \cos\beta y \quad 0\le x\le a;\ 0\le y\le b; \tag{16b}$$

$$w_0(x,y) = \sum_{m=1}^{\infty}\sum_{n=1}^{\infty} W_{mn} \sin\alpha x \sin\beta y\ e^{-i\omega t}\ , \ 0\le x\le a;\ 0\le y\le b; \tag{16c}$$

$$\theta_x(x,y) = \sum_{m=1}^{\infty}\sum_{n=1}^{\infty} X_{mn} \cos\alpha x \sin\beta y \ , \ 0\le x\le a;\ 0\le y\le b; \tag{16d}$$

$$\theta_y(x,y) = \sum_{m=1}^{\infty}\sum_{n=1}^{\infty} Y_{mn} \sin\alpha x \cos\beta y\ e^{-i\omega t}\ , \ 0\le x\le a;\ 0\le y\le b; \tag{16e}$$

$$\theta_z(x,y) = \sum_{m=1}^{\infty}\sum_{n=1}^{\infty} Z_{mn} \sin\alpha x \sin\beta y \ , \ 0\le x\le a;\ 0\le y\le b; \tag{16f}$$

$$u_0^*(x,y) = \sum_{m=1}^{\infty}\sum_{n=1}^{\infty} U_{mn}^* \cos\alpha x \sin\beta y \ , \ 0\le x\le a;\ 0\le y\le b; \tag{16g}$$

$$v_o^*(x,y) = \sum_{m=1}^{\infty}\sum_{n=1}^{\infty} V_{mn}^* \sin\alpha x \cos\beta y \ , \ 0\le x\le a;\ 0\le y\le b; \tag{16h}$$

$$w_0^*(x,y) = \sum_{m=1}^{\infty}\sum_{n=1}^{\infty} W_{mn}^* \sin\alpha x \sin\beta y \ , \ 0\le x\le a;\ 0\le y\le b; \tag{16i}$$

$$\theta_x^*(x,y) = \sum_{m=1}^{\infty}\sum_{n=1}^{\infty} X_{mn}^* \cos\alpha x \sin\beta y \ , \ 0\le x\le a;\ 0\le y\le b; \tag{16j}$$

$$\theta_y^*(x,y) = \sum_{m=1}^{\infty}\sum_{n=1}^{\infty} Y_{mn}^* \sin\alpha x \cos\beta y \ , \ 0\le x\le a;\ 0\le y\le b; \tag{16k}$$

$$\theta_z^*(x,y) = \sum_{m=1}^{\infty}\sum_{n=1}^{\infty} Z_{mn}^* \sin\alpha x \sin\beta y \ , \ 0\le x\le a;\ 0\le y\le b; \tag{16l}$$

The eigen problem related to governing equations is defined as

$$([S]_{9\times 9} - \lambda[\varsigma]_{9\times 9})\mathbf{X} = 0 \tag{17}$$

Where [S] collects all stiffness terms and $[\varsigma]$ collects all terms related to the in-plane forces. In Equation (17) **X** are the modes of buckling associated with the buckling loads defined as λ. For each value of m and n, there is a unique value of N_{cr}. The critical buckling load is the smallest value of $N_{cr}(m, n)$.

4. Results and discussion

4.1. Comparative studies

To validate the accuracy of the present higher order theory in predicting the critical buckling load of FG plates subjected to different in-plane loading conditions (Uniaxial compression: $\lambda_1 = -1, \lambda_2 = 0;$ biaxial compression: $\lambda_1 = -1, \lambda_2 = -1;$ biaxial compression and tension $\lambda_1 = -1, \lambda_2 = 1$), three numerical examples are presented and discussed. The material properties adopted here are :
Aluminium Young's modulus (E_m)= 70GPa, density ρ_m= 2702 kg/m^3, and Poisson's ratio (υ)= 0.3; Alumina Young's modulus (E_c)= 380GPa, density ρ_c= 3800kg/m^3, and Poisson's ratio (υ)= 0.3.

For convenience, the critical buckling load is presented in nondimensionalized form as:

$$\overline{N} = N_{cr} \frac{a^2}{E_m h^3} \tag{18}$$

Example 1.

The first comparison is carried out for simply supported FG plate subjected to uniaxial compression along the x-axis ($\lambda_1 = -1, \lambda_2 = 0$) The comparisons of nondimensionalized critical buckling loads ($\overline{N}$) obtained by present theory and those given by Thai and Choi [27] is presented in Table 1. It can be observed that, the effect of thickness stretching is lowering the critical buckling loads compared to the results of Thai and Choi [27]. It can also be seen that, the critical buckling load decreases with the increase of power-law index value while it increases with the increase of aspect ratio. Furthermore, increasing of thickness ratio, aspect ratio, not only increases the critical buckling load values, but also causes the changes in critical buckling modes at aspect ratio value is 1.5 and 2 when thickness stretching effect is not considered and only one buckling mode is exist when thickness stretching effect is considered.

Table 1. Comparison of nondimensionalized critical buckling load ($\overline{N}$)of simply supported Al/Al2O3 plate subjected to uniaxial compression along x-axis ($\lambda_1 = -1, \lambda_2 = 0$)

		Power law index (n)			
a/b		0	0.5	1	10
0.5	Ref.[27]	7.4053	4.8206	3.7111	2.1896
	Present	7.37802	4.80131	3.69368	2.1785
1	Ref.[27]	18.5785	12.1229	9.3391	5.4528
	Present	18.4721	12.0473	9.27091	5.4104
1.5	Ref.[27]	40.7476[a]	26.9091[a]	20.8024[a]	11.5379[a]
	Present	47.0557	30.7961	23.7109	13.613
2	Ref.[27]	64.0842[a]	42.5015[a]	32.898 [a]	17.9227[a]
	Present	106.144	69.7804	53.764	30.233

[a]Mode for plate is (m, n)=(2, 1)

Example 2.

The next comparison is performed for the simply supported FG plate subjected to inplane biaxial compression ($\lambda_1 = -1, \lambda_2 = -1$). The results of critical buckling loads obtained by

present theory and those reported by Thai and Choi [27] are presented in Table 2 and observed that the critical buckling loads are higher when thickness stretching is neglected comapared to the present results. It can be seen that, in this loading condition also, the nondimensionalized critical buckling load decreases with the increase of power-law index, while increases with the increase of aspect ratio, but only one critical buckling mode exists in any case of the aspect ratio, thickness ratio and modulus ratio, and power-law index.

Table 2. Comparison of nondimensionalized critical buckling load ($\overline{N}$) of simply supported Al/Al2O3 plate subjected to biaxial compression ($\lambda_1 = -1,\ \lambda_2 = -1$)

		Power law index (n)			
a/b		0	0.5	1	10
0.5	Ref. [27]	5.9263	3.8565	2.9689	1.7517
	Present	5.9024	3.841	2.9549	1.74276
1	Ref. [27]	9.2893	6.0615	4.6696	2.7264
	Present	9.236	6.0237	4.6355	2.7052
1.5	Ref. [27]	14.608	9.5685	7.3793	4.2384
	Present	14.479	9.4757	7.2957	4.1885
2	Ref. [27]	21.505	14.1552	10.9323	6.1481
	Present	21.229	13.956	10.753	6.04668

Example 3.

The last comparison is carried out for the simply supported FG plates under inplane biaxial compression and tension ($\lambda_1 = -1, \lambda_2 = 1$). The results predicted by present theory are compared with the Thai and Choi [27] results and seen that the present theory results are lower due to thickness stretcing effect. The results are presented in Table 6.3. It can also be seen that, under biaxial compression and tension also, the critical buckling load decreases with the increase of power-law index value while it increases with the increase of aspect ratio, same as in uniaxial and biaxial compression. Also, increasing of thickness ratio, aspect ratio, not only increases the critical buckling load values, but also causes the changes in critical buckling modes. This can be observed when aspect ratio value is 1. The critical buckling mode varies from (2,1) to (1,2).

Table 3. Comparison of nondimensionalized critical buckling load($\overline{N}$) of simply supported Al/Al2O3 plate subjected to biaxial compression and tension($\lambda_1 = -1, \lambda_2 = -1$)

		Power law index (n)			
a/b		Ceramic	0.5	1	10
0.5	Ref. [27]	9.8738	6.4275	4.9481	2.9195
	Present	9.83737	6.40174	4.9249	2.9046
1	Ref. [27]	35.8461[a]	23.5920[b]	18.2206[a]	10.2468[a]
	Present	35.3812[a]	23.2603[b]	17.9215[a]	10.0781[a]
1.5	Ref. [27]	37.9819	24.8781	19.1863	11.0199
	Present	37.6446	24.6369	18.9687	10.8901
2	Ref. [27]	35.8416	23.592	18.2206	10.2468
	Present	35.3812	23.2601	17.9213	10.0778

[a]Mode for plate is (m, n)=(2, 1)
[b]Mode for plate is (m, n)=(1, 2)

4.2. Parametric study

The effect of side-to-thickness ratio, aspect ratio and the modulus ratio of nondimensionalized critical buckling load for simply supported FG plate made of Al/Al_2O_3 with $\varepsilon_z \neq 0$ is investigated. Figure 2 - Figure 4 represents the variation of nondimensionalized critical buckling load with side-to-thickness ratio, aspect ratio and modulus ratio respectively under uniaxial compression. It is important to observe that, the effect of shear deformation and bending-extensional coupling is most for metals and least for ceramics and also the shear deformation effect is felt for a/h≤10, aspect ratio a/b≤1.5 and for modulus ratio E_m/E_c =0.5. Also it is shown that, increase of side-to-thickness ratio and aspect ratio and power-law index values, increases the nondimensionalized critical buckling load while it decreases with increase of modulus ratio.

The effect of side-to-thickness ratio, aspect ratio, modulus ratio and power law index values on nondiensionalized critical buckling load for a simply supported FG plate under biaxial compression is shown in Figure 5 - Figure 7. The same can be observed as in the case of uniaxial compression. It is important to observe that, the critical buckling loads are larger in uniaxial compression and smaller in biaxial compression. Figure 8 shows the variation of nondimensionalized critical buckling load of different modulus ratios and power law index values under inplane compression and tension. It can be observed that, critical buckling load decreases with the increase of modulus ratio and power-law index values.

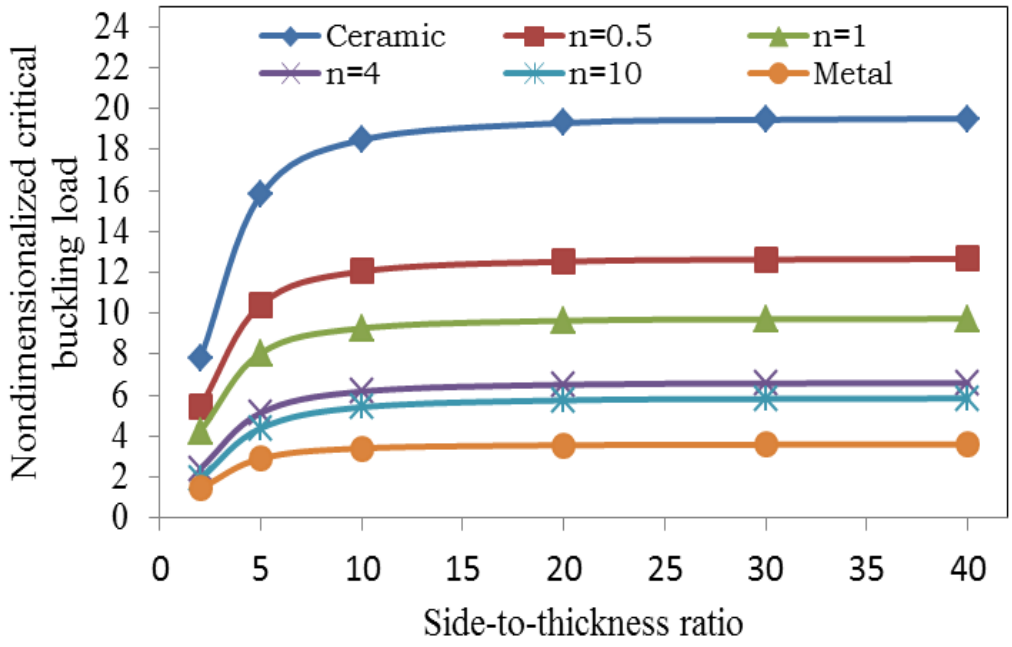

Figure 2. Effect ofside to thickness ratios(a/h) on nondimensionalized critical buckling load ($\overline{N}$)under uniaxial compression for a simply supported FG plate for various materialvariation parameters(n)

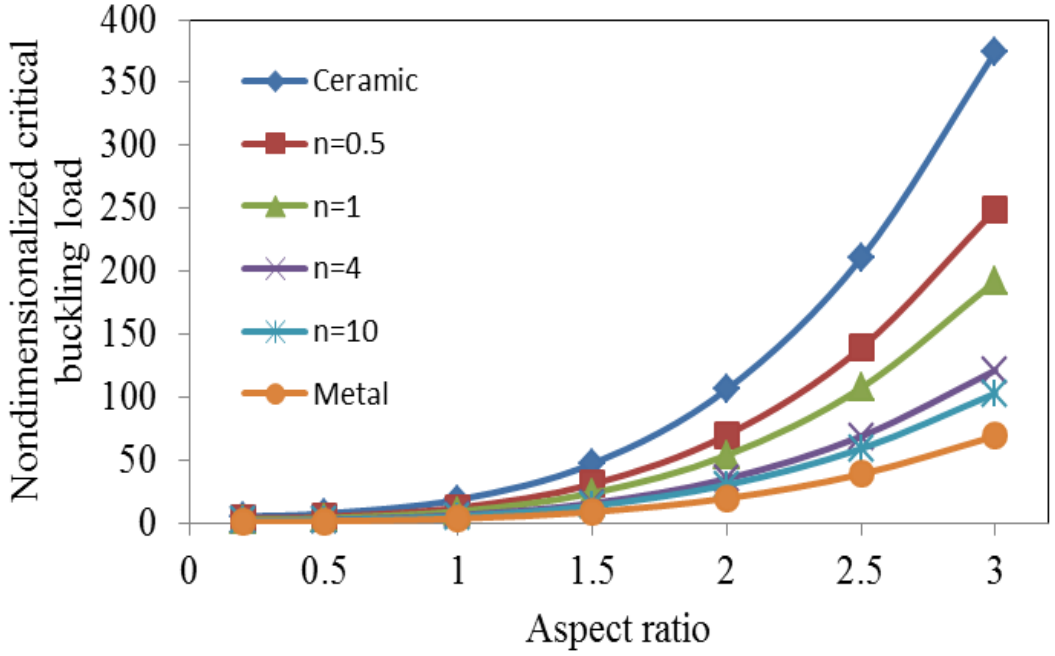

Figure 3. Effect of aspectratios(a/b) on nondimensionalized critical buckling load ($\overline{N}$) under uniaxial compression for a simply supported FG plate for various material variation parameters(n)

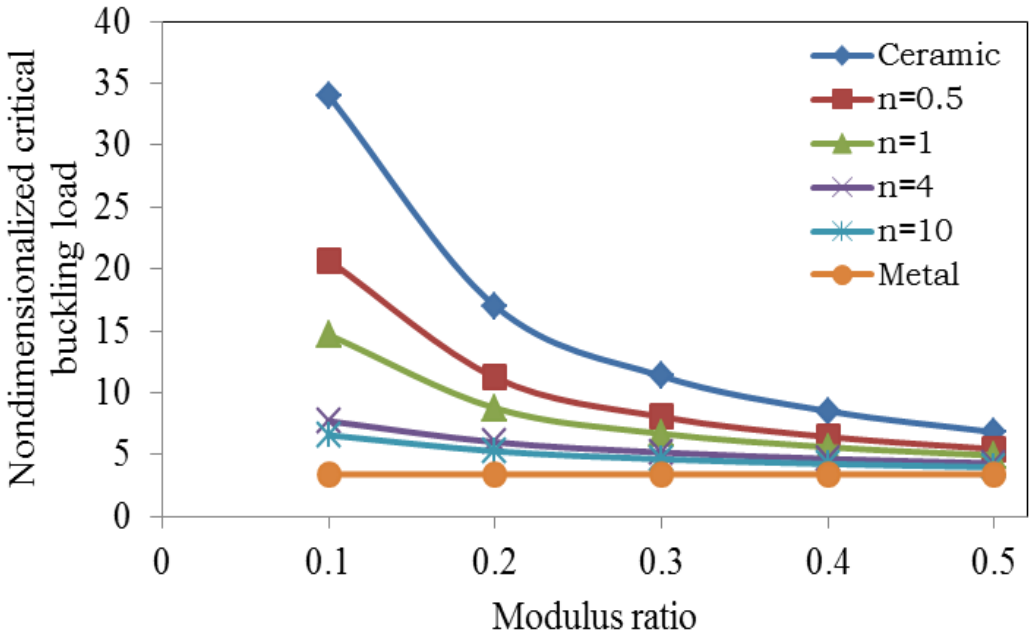

Figure 4. Effect of modulus ratio (E_m/E_c) on nondimensionalized critical buckling load ($\overline{N}$) under uniaxial compression for a simply supported FG plate for various material variation parameters(n)

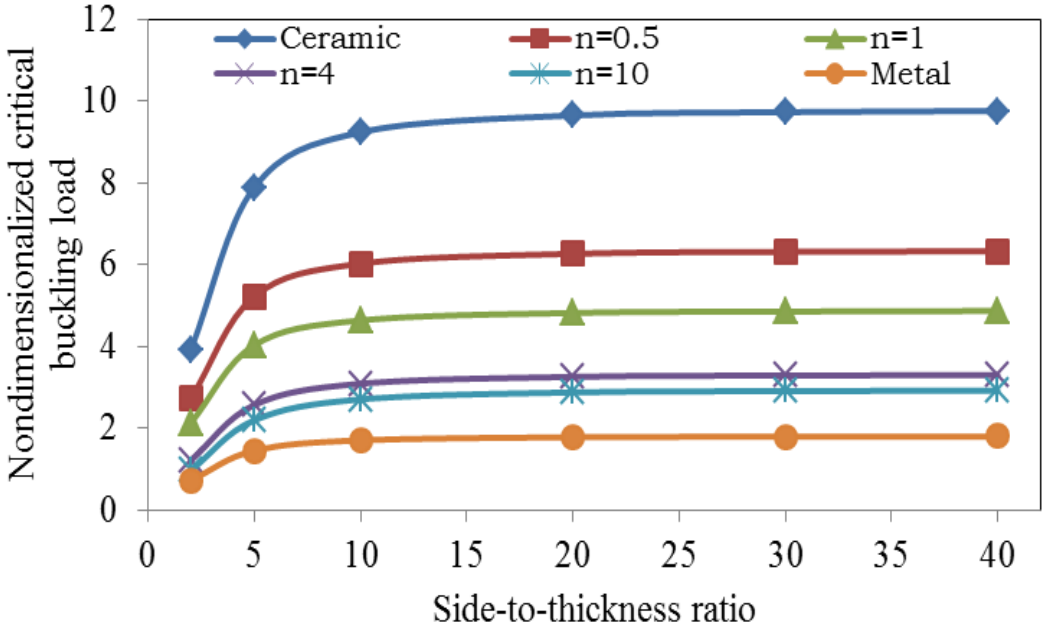

Figure 5. Effect ofside to thickness ratios(a/h) on nondimensionalized critical buckling load ($\overline{N}$) under biaxial compression for a simply supported FG plate for various material variation parameters(n)

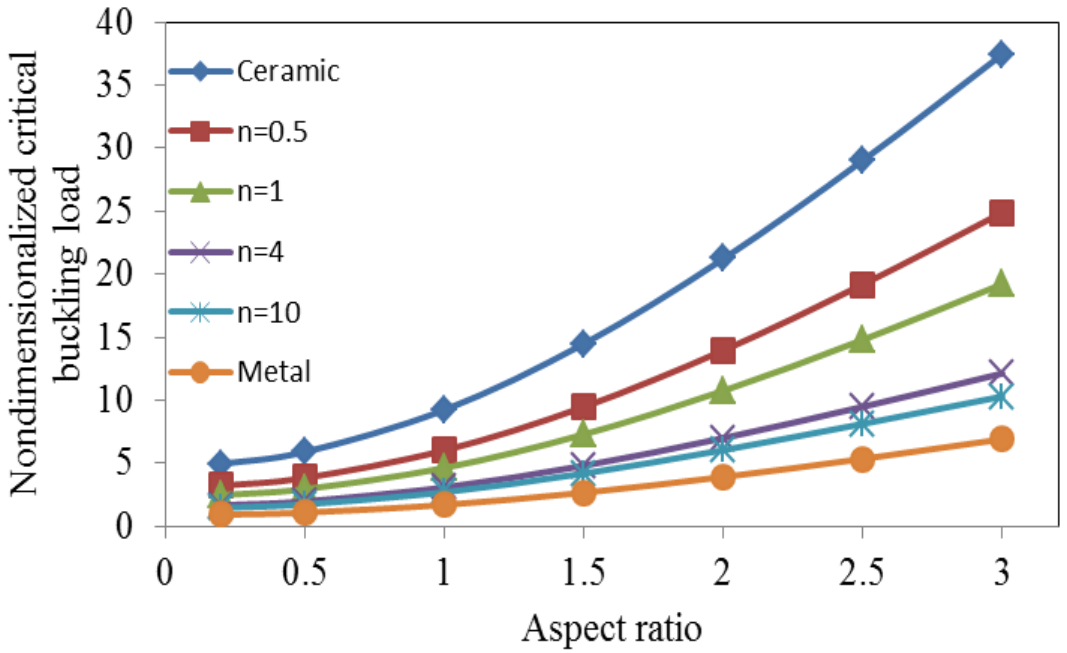

Figure 6. Effect ofaspect ratios(a/b) on nondimensionalized critical buckling load ($\overline{N}$) under biaxial compression for a simply supported FG plate for various material variation parameters(n)

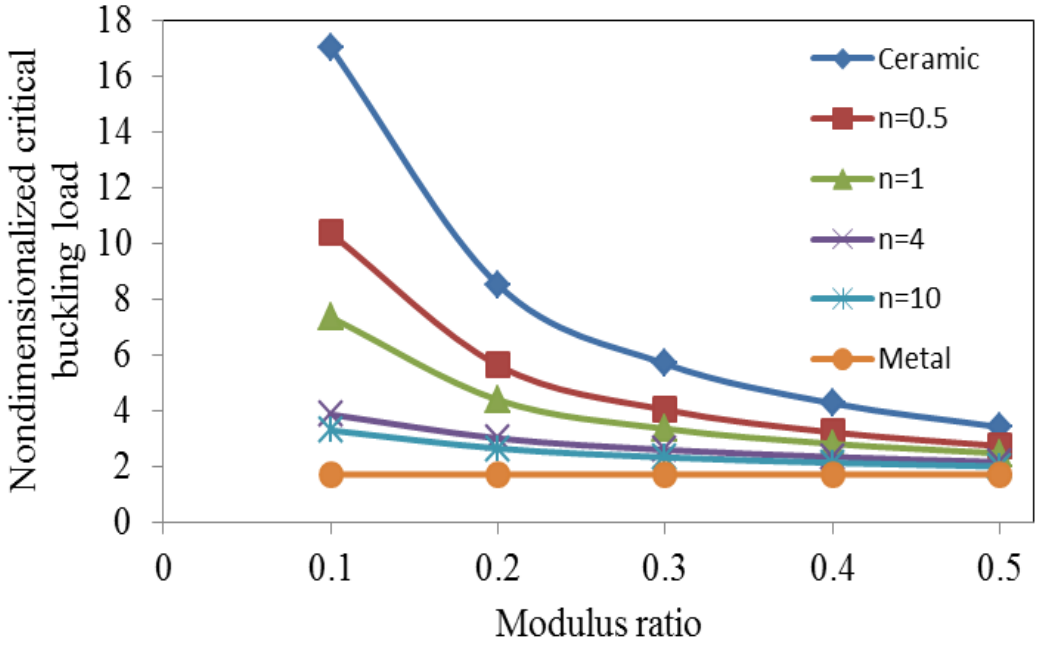

Figure 7. Effect ofmodulus ratios(E_m/E_c) on nondimensionalized critical buckling load ($\overline{N}$) Under biaxial compression for a simply supported FG plate for various material variation parameters(n)

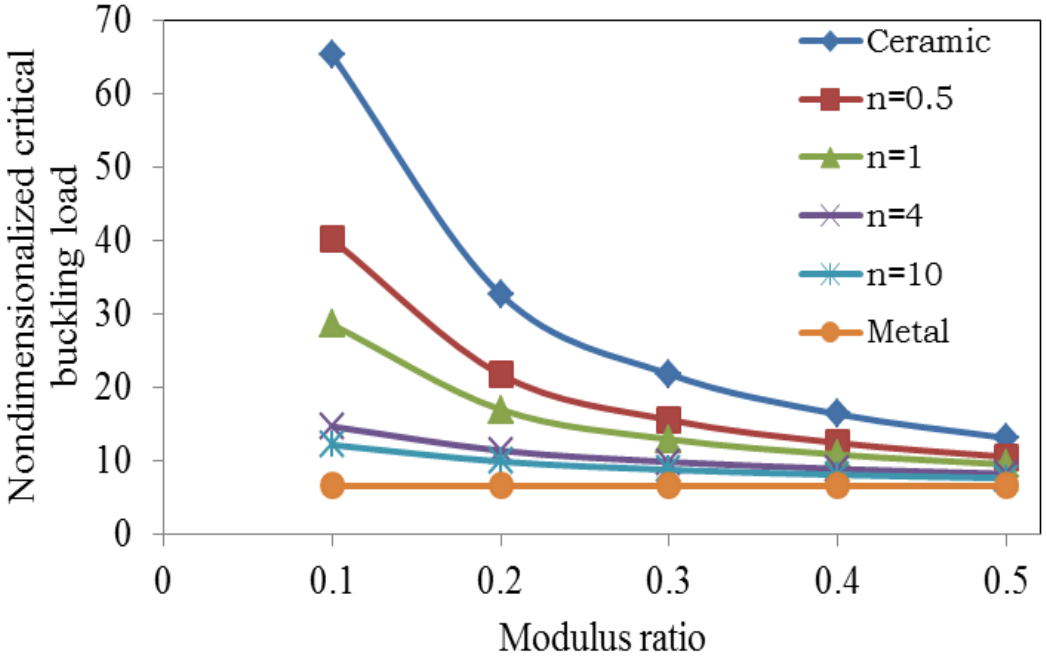

Figure 8. Effect ofmodulus ratios(E_m/E_c) on nondimensionalized critical buckling load ($\overline{N}$)under biaxial compression and tension for a simply supported FG plate for various material variation parameters(n)

5. Conclusions

A higher order shear deformation theory with thickness stretching effect was successfully developed and applied to study the buckling behavior of functionally graded plates without enforcing zero transverse shear stresses on the top and bottom surfaces of the plate. The present formulation was compared with the refined theory developed by Thai and Choi[27] and the effect of thickness stretching is observed.This eliminated the need of using shear correction factors. It can be concluded that for getting the more improved results for buckling the thickness stretching effect should be included in the development of the higher order theory for simply supported FG plates. Hence, the present findings will be useful benchmark for evaluating the other future plate theories and numerical methods such as the finite element and meshless methods.

References

[1] Javaheri, R. and Eslami, M. R. 2002. Buckling of functionally graded plates under in-plane compressive loading. *Journal of Applied Mathematics and Mechanics*, 82, 4: 277-283.

[2] Abrate, S. 2008. Functionally graded plates behave like homogeneous plates. *Composites part B*, 38, 1: 151-158.

[3] Mohammadi, M., Saidi, A.R., and Jomehzadeh, E. 2010. Levy solution for buckling analysis of functionally graded rectangular plates. *Applied Composite Materials*, 17, 2: 81-93.

[4] Mahdavian, M. 2009. Buckling analysis of simply supported functionally graded rectangular plates nunder non-uniform in-plane compressive loading. *Journal of Solid Mechanics*, 1, 3: 213-225.

[5] Feldman, E. and Aboudi, J. 1997. Buckling analysis of functionally graded plates subjected to uniaxial loading. *Composite Structures*, 38, 1-4: 29-36.

[6] Samsam Shariat, B. A., Javaheri, R., and Eslami, M. R. 2005. Buckling of imperfect functionally graded plates under in-plane compressive loading. *Thin-Walled Structures*, 43, 7:1020-1036.

[7] Tung, H. V. and Duc, N. D. 2010. Nonlinear analysis of stability for functionally gradedplates under mechanical and thermal loads. *Composite Structures*, 92, 5:1184-1191.

[8] Reissner, E. 1945. The effect of transverse shear deformation on the bending of elastic plates. *ASME Journal of Applied Mechanics*, 12, 2: 69-77.

[9] Mindlin, R. D. 1951. Influence of rotary inertia and shear on flexural motions of isotropic, elastic plates. *ASME Journal of Applied Mechanics*, 18: 31-38.

[10] Thai, H. T. and Vo, T. P. 2013. A new sinusoidal shear deformation theory for bending, buckling, and vibration of functionally graded plates. *Applied mathematical modelling*, 37: 3269-3281.

[11] Yang, J., Liew, K.M., and Kitipornchai, S. 2005. Second-order statistics of the elastic buckling of functionally graded rectangular plates. *Composites Science and Technology*, 65, 7–8: 1165-1175.

[12] Mohammadi, M., Saidi, A. R., and Jomehzadeh, E. 2009. A novel analytical approach for the buckling analysis of moderately thick functionally graded rectangular plates with two simply-supported opposite edges", *Proceedings of IMechE Part C: Journal of Mechanical Engineering Science*, 224: 1831-1841.

[13] Zhao, X., Lee, Y. Y., and Liew, K. M. 2009. Mechanical and thermal buckling analysis of functionally graded plates. *Composite Structures*, 90, 2: 161-171.

[14] Sepiani, H. A., Rastgoo, A., Ebrahimi, F., and Ghorbanpour Arani, A. 2010. Vibration and buckling analysis of two-layered functionally graded cylindrical shell, considering the effects of transverse shear and rotary inertia. *Materials & Design*, 31, 3: 1063-1069.
[15] Naderi, A. and Saidi, A R. 2010. On pre-buckling configuration of functionally graded Mindlin rectangular plates. *Mechanics Research Communications*, 37, 6: 535-538.
[16] Saha, R. and Maiti. P.R. 2012. Buckling of simply supported FGM plates under uniaxial load. *International Journal of Civil and Structural Engineering*, 2, 4:1036-1050.
[17] Javaheri, R. and Eslami, Mr. 2002. Thermal buckling of functionally graded plates based on higher order shear deformation theory. *Journal of Thermal stresses*, 25, 7: 603-625.
[18] Najafizadeh, M. M. and Heydari, H. R. 2004. Thermal buckling of functionally graded circular plates based on higher order shear deformation plate theory. *European Journal of Mechanics - A/Solids*, 23, 6: 1085-1100.
[19] Bodaghi, M. and Saidi, A. R. 2010. Levy-type solution for buckling analysis of thickfunctionally graded rectangular plates based on the higher-order shear deformation plate theory. *Applied Mathematical Modelling*, 34, 11: 3659-3673.
[20] Bagherizadeh, E., Kiani, Y., and Eslami, M. R. 2011. Mechanical buckling of functionally graded materialcylindrical shells surrounded by Pasternak elastic foundation. *Composite Structures*, 93, 11: 3063-3071.
[21] Mozafari, H. and Ayob, A. 2012. Effect of Thickness Variation on the Mechanical Buckling Load in Plates Made of Functionally Graded Materials. *Procedia Technology*, 1:496-504.
[22] Ma, L. S, and Wang, T. J. 2003. Nonlinear bending and post-buckling of a functionally graded circular plate under mechanical and thermal loadings. *International Journal of Solids and Structures*, 40, 1-14: 3311-3330.
[23] Hosseini-Hashemi, S., Khorshidi, K., and Amabili, M. 2008. Exact solution for linear buckling of rectangular Mindlin plates. *Journal of Sound and Vibration*, 315: 318-342.
[24] Saidi, A.R., Rasouli, A, and Sahraee, S. 2009. Axisymmetric bending and buckling analysis of thickfunctionally graded circular plates using unconstrained third-order shear deformation plate theory. *Composite Structures*, 89, 1: 110-119.
[25] Oyekoya, O. O. Mba, D. U., and El-Zafrany, A.M. 2009. Buckling and vibration analysis of functionally graded composite structures using the finite element method. *Composite Structures*, 89, 1: 134- 142
[26] Ghannadpour, S. A. M., Ovesy, H. R., and Nassirnia, M. 2012. Buckling analysis of functionally graded plates under thermal loadings using the finite strip method. Computers & Structures, 108—109: 93-99
[27] Thai, H. T. and Choi, D. H. 2012. An efficient and simple refined theory for buckling analysis of functionally graded plates. *Applied Mathematical Modelling*, 36: 1008-1022.
[28] Uymaz, B. and Aydogdu, M. 2013. Three dimensional mechanical buckling of FG plates with general boundary conditions. *Composite Structures*, 96: 174-193.
[29] Lal, A., Jagtap, K.R., and Singh, B.N. 2013. Post buckling response of functionally graded materials plate subjected to mechanical and thermal loadings with random material properties. *Applied Mathematical Modelling*, 37, 5-1: 2900-2920.